ACADEMIA ROMÂNĂ
Revue Roumaine de Chimie
http://web.icf.ro/rrch/

Rev. Roum. Chim.,
2015, *60*(11-12), 1033-1037

THE PEAT – TEMPLATE AGENT FOR Ni FERRITE OBTAINMENT

Anca Mihaela DUMITRESCU,[a] Victor JUCAN,[b] Lacramioara RUSU,[c]
Alexandra Raluca IORDAN[a,*] and Mircea Nicolae PALAMARU[a]

[a] Faculty of Chemistry, Alexandru Ioan Cuza University of Iaşi, 11, Carol I Boulevard, 700506, Iaşi, Roumania
[b] Faculty of Geography and Geology, Alexandru Ioan Cuza University of Iaşi, 20A, Carol I Boulevard, 700505, Iaşi, Roumania
[c] Faculty of Engineering, Vasile Alecsandri University of Bacău, 157, Mărăşeşti Street, 600115, Bacău, Roumania

Received January 15, 2015

Ni ferrite of spinel type was synthesized by sol-gel autocombustion method using brown peat as template agent. The structure of as-obtained sample was investigated by IR, XRD and SEM. It was found that synthesized Ni ferrite has a spongy porous structure of cubic spinel-type and the particle size is of nanometer order (36 nm). The obtained Ni ferrite obtained will be subject to some catalytic tests in order to determine their efficiency in processes of phenol decomposition.

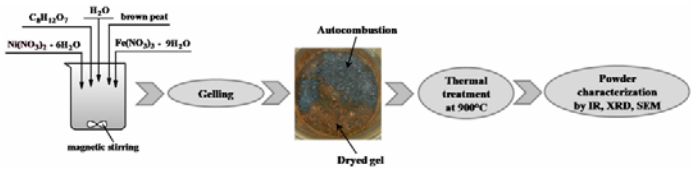

INTRODUCTION

Ni ferrite is a porous magnetic material largely used in electronics and telecommunication industries.[1] This ferrite in a typical inverse spinel compound, in which Fe^{3+} ions are placed on tetrahedral sites and Ni^{2+} ions are placed on octahedral sites only.[2] Properties of Ni ferrite have been intensively studied due to their porosity. To improve the porosity and magnetic properties of Ni ferrite, some synthesis methods were studied such as co-precipitation,[3] sol-gel autocombustion,[4] hydrothermal,[5] plasma or microwave procedures,[6, 7] microemulsion.[8]

In the last decade, scientists have tried improving existing methods or finding new synthesis methods for obtaining $NiFe_2O_4$ with high porosity, pre-established microstructure and size crystallites under 50 nm. It is known that high porosity and small size crystallites provides high specific surface area and selectivity, properties that represent key qualities for catalysts and sensors for example. In this purpose, a host template method was developed. This synthesis method involves using a classical material microstructure, which plays the role of template agent. Studies carried out to data have shown that wood,[9] cellulose,[4] silica,[10] a variety of polymers[11] can be used as template agent for obtaining of ferrites with superior properties. So, S.C. Kiong *et al*[9] have obtained MnZn ferrite using wood as template agent. Kiong has observed that the ferrite crystallites "grow" on the wood typical microstructure. A.M. Dumitrescu *et al*[4] have obtained Ni ferrite using cellulose as template agent. It has been observed that crystallites "grow" on the cellulose microfibers. Moreover, authors observed that this type of aggregation prevents agglomeration.

Other material that may be used as template agent is the peat. Peat is a porous organic material with variable composition that depends on the source, the nature of basic vegetation, the degree of metamorphosis.[12]

The present study analyzes the results obtained for Ni ferrite synthesized by sol-gel autocombustion method using citric acid as chelating/fuel and peat as template agent.

* Corresponding author: alexandra.iordan@uaic.ro

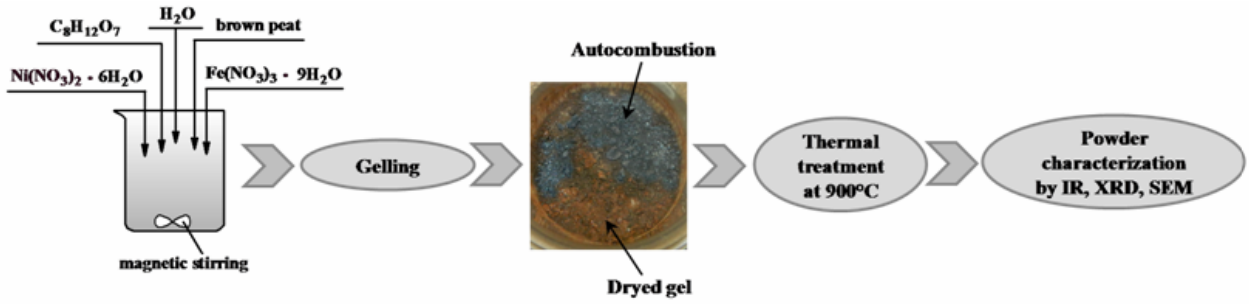

Fig. 1 – Protocol synthesis of Ni ferrite.

EXPERIMENTAL

All chemical reagents (Merk) were used without further purifications.

Ni ferrite was synthesized by sol-gel autocombustion method using citric acid ($C_8H_{12}O_7$) as chelating/fuel agent. $Ni(NO_3)_2$ hexahydrate and $Fe(NO_3)_3$ nonahydrate was used as cation sources. Atomic ratio of metal cations Ni^{2+} : Fe^{3+} = 1:2. Ferrite:citric acid mass ratio is 1:3. Brown peat collected from Covasna region, Romania, was used as template agent. Ferrite:peat mass ratio is 2:1. Synthesis protocol is presented in Fig. 1.

Details about synthesis process were described elsewhere.[4]

The as-obtained samples were characterized by IR, XRD, SEM and BET-specific surface area. IR spectra were recorded in the mid infrared range (4000 – 300 cm^{-1}) with Fourier transform (FTIR) using a Bruker spectrophotometer TENSOR^{TM} 27-type with an anvil ATR cell and a resolution of 2 cm^{-1}. X-ray diffraction (XRD) patterns were recorded with a Shimadzu LabX 6000 instrument equipped with a graphite monochromator using a Cu K_α radiation (λ=0.15406 nm). SEM images were obtained in a Quanta 200 apparatus with EDAX system of elemental analysis. BET-specific surface area of as-obtained Ni-ferrite was achieved from N_2-sorption experiments. A known mass of sample was first thermally treated under vacuum at 473 K. Isotherm was collected at 77 K using a Quantachrome Nova 2200 surface analyzer instrument. The Brunauer–Emmet–Teller (BET) method was used to calculate the specific surface area.

RESULTS AND DISCUSSION

Characterization of peat

Elemental composition of brown peat used as template agent in this study is presented in Table 1.

It can be observed that brown peat has a high content of carbon. This means that brown peat used in our work contain a significant mineral phase.[14]

SEM analysis (Fig. 2) shows that brown peat is a spongy porous material with agglomerated particles. These agglomerates are spread uniformly all over mass of the sample.[13, 14]

Characterization of ferrite

IR spectra for as-obtained ferrite is shown in Fig. 3. No absorbtion bands characteristic to nitrate or carbonate groups was observed. Consequently, a wavelengh range between 1000 – 300 cm^{-1} was selected for these spectra. Over this wavelengh range, only characteristic bands of spinel structure were identified, as also confirmed by XRD analysis.

The high amplitude absorption band from 561 cm^{-1} was assigned to the lattice vibrations corresponding to the Fe^{3+} – O^{2-} links from the tetrahedral positions (A). Absorption bands from 470 to 420 cm^{-1} can be assigned to the asymmetrical vibrations of the lattice corresponding to Ni^{2+} – O^{2-} bonds. In 400 – 350 cm^{-1} range were identified low amplitude absorption bands assigned to the lattice vibrations of the corresponding Fe^{3+} – O^{2-} bonds from octahedral positions [B].

X-ray diffraction. XRD pattern for sample analyzed is shown in Fig. 4. The diffraction peaks were identified in agreement with the referred database of the International Centre for Diffraction Data (ICDD).[15] The characteristic diffraction peak for spinel cubic structure belonging to (311) Miller plane and corresponding to the Fd3m space group was identified at $2\theta \approx 36°$.

Table 1

Elemental analysis for brown peat

Characteristic	Brown peat
C (%)	39.65
H (%)	4.32
N (%)	2.27
Total P_2O_5 (%)	0.20
Organic matter (%)	71.38

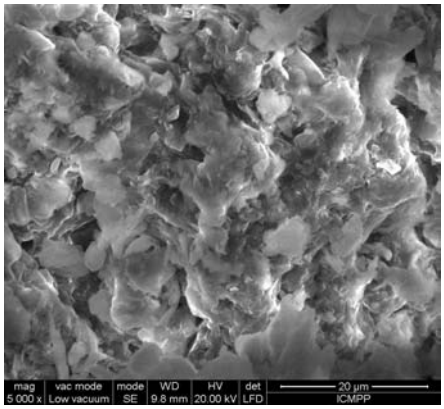

Fig. 2 – Electronic micrography for brown peat.

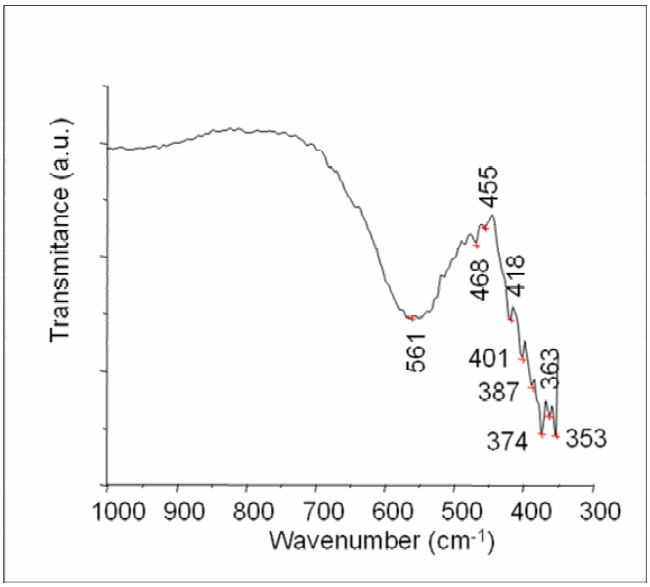

Fig. 3 – IR spectra for Ni ferrite thermally treated at 900°C.

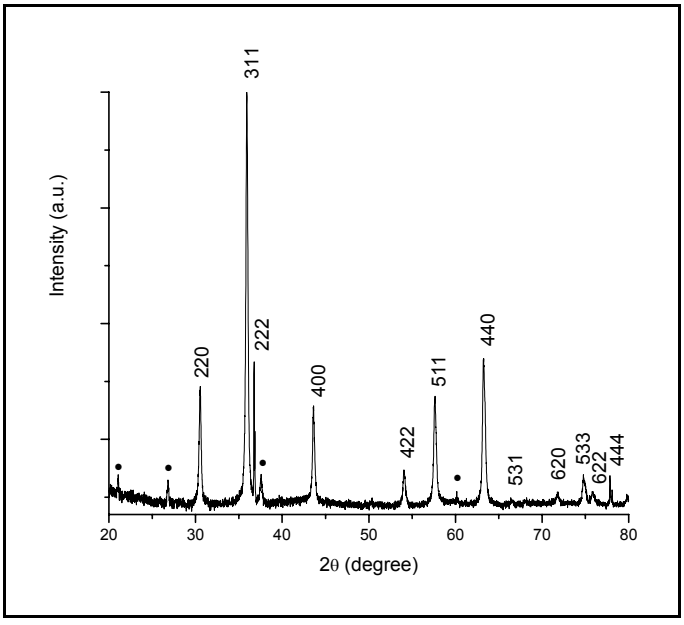

Fig. 4 – XRD pattern for Ni ferrite thermally treated at 900°C.

Besides the characteristic diffraction lines of nickel ferrite obtained, additional diffraction lines appear (noted as black bullet in Figure), attributed to the secondary phase identified as brown peat.[14]

XRD analysis provided the following crystallographic data. The crystallite size, D_c, was calculated using Scherrer's relation:[16]

$$D_c = \frac{0.94\lambda}{\beta_{1/2}\cos\theta} \qquad \text{Eq. (1)}$$

where λ = 1.5405 Å; $\beta_{1/2}$ – peak width at half-maximum intensity (degrees).

The lattice parameter, *a*, was obtained with relation:[17]

$$a = d_{hkl}\sqrt{\left(h^2 + k^2 + l^2\right)} \qquad \text{Eq. (2)}$$

where d_{hkl}, the distance between the adjacent Miller planes (h k l), is calculated from Bragg relation:

$$d_{hkl} = n\lambda/2\sin\theta \qquad \text{Eq. (3)}$$

with n = 1 for the cubic system.

To determine the crystallite sizes, 3 intense diffraction lines, which had been deconvoluted to Gaussian curves, have been mainly employed, while the crystallite size was determined using full-width at half-maximum value. So, from calculations results for crystallite size D_c = 36 nm and lattice parameter a = 8.35.

Other information obtained from XRD data were the interionic distances and the distribution of cations among tetrahedral and octahedral sites of spinel lattice.

Using the value of lattice parameter is possible to calculate the value of the interionic distances and the mean ionic radius per molecule of the tetrahedral and octahedral sites, r_{tetr} and r_{oct}. The results are shown in Table 2. Details about relations of calculus used were described elsewhere.[18]

Using these results, the cation distribution of Ni ferrite synthesized using brown peat as a template agent was determined. So, for analyzed sample we can propose the following general formula: $\left(Fe^{3+}\right)^{[4]}\left[Ni^{2+}Fe^{3+}\right]^{[6]}O_4$. This formula indicated that the Fe^{3+} ions have migrated from the B to A sites. Iron can occupy both the tetrahedral (A) and the octahedral [B] positions in the cubic spinel structure, while Ni^{2+} ions show a strong preference for octahedral site. Also, this formula for cation distribution showed that the obtained Ni ferrite has an inverse spinel structure.[19]

Electronic microscopy and BET-specific surface area. SEM micrography for the analyzed sample is shown in Fig. 5.

Table 2

Interionic distance for Ni ferrite termally treated at 900°C

Interionic distance	Results
Cation–anion distances at A-site (d_{AL})	1.80
Cation–anion distances at B-site (d_{BL})	2.08
Distance of closest anion–anion approach, tetrahedral edge, d_{AE}	2.95
Shared octahedral edges, d_{BE}	2.95
Unshared octahedral edges, d_{BEU}	2.95
Radius of the ions at tetrahedral site, r_{tetr}	0.48
Radius of the ions at octahedral site, r_{oct}	0.76

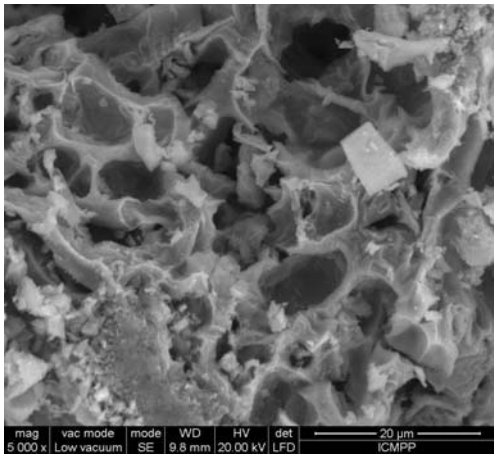

Fig. 5 – SEM micrography for Ni ferrite thermally treated at 900°C.

It can be observed that Ni ferrite analyzed sample shows a spongy porous microstructure. This microstructure can be attributed to the brown peat used as template agent (see Fig. 2). On the other hand, brown peat influences significantly the combustion process that occurred slowly and for a longer period of time (maximum 40 min), which ensures sufficient time for the orientation of ferrite crystallites within the spaces created by brown peat.

Specific surface areas, S_{BET}, calculated from the adsorption of nitrogen, show that the Ni ferrite nanopowders are formed by nanoparticles agglomerates with relatively high surface area, 44 m^2/g. This result recommended the as-obtained Ni ferrite using brown peat as a template agent for the catalytic applications such as processes of phenol decomposition.

CONCLUSIONS

The effect of brown peat on the structure of Ni ferrite has been investigated.

Ni ferrite of spinel type with spongy porous structure was confirmed by XRD and SEM analysis.

The as-obtained sample has an inverse spinel structure with general formula for cation distribution $\left(Fe^{3+}\right)^{[4]}\left[Ni^{2+}Fe^{3+}\right]^{[6]}O_4$, indicating that the Fe^{3+} ions have migrated from the octahedral [B] to the tetrahedral (A) positions in the cubic spinel structure.

The as-obtained Ni ferrite will be subject to some catalytic tests in order to determine its efficiency in processes of phenol decomposition.

Acknowledgments: Victor Jucan thanks for the financial support provided by POSDRU/159/1.5/S/133652.

REFERENCES

1. M. R. Barati, S. A. Seyyed Ebrahimi and A. Badiei, *J. Non-Cryst. Solids.*, **2008**, *354*, 5184-5185.
2. D. T. T. Nguyet, N. P. Duong, L. T. Hung, T. D. Hien and T. Satoh, *J. Alloy. Compd.*, **2011**, *509*, 6621-6625.
3. M. M. Rashad and O. A. Fouad, *Mater. Chem. Phys.*, **2005**, *94*, 365-370.
4. A. M. Dumitrescu, P. M. Samoila, V. Nica, F. Doroftei, A. R. Iordan and M. N. Palamaru, *Powder Technol.*, **2013**, *243*, 9-17.
5. L. Lv, J. P. Zhou, Q. Liu, G. Zhu, X. Z. Chen, X. B. Bian and P. Liu, *Physica E*, **2011**, *43*, 1798-1803.
6. A. M. Bhavikatti, S. Kulkarni and A. Lagashetty, *Int. J. Eng. Sci. Technol.*, **2011**, *3(1)*, 687695.
7. K. Zehani, F. Mazaleyrat, V. Loyau and E. Laboure, *J. Appl. Phys.*, **2011**, *109(7)*, 07A504-07A504-3.
8. R. D. K. Misra, A. Kale, B. J. Kooi and J. Th. M. De Hosson, *Mater. Sci. Technol.*, **2003**, *19*, 1617-1621.
9. S. C. Kiong, D. Mutou, N. Adachi and T. Ota, *J. Aust. Ceram. Soc.*, **2009**, *45(2)*, 34-39.
10. T. Valdes-Solis, P. Tartaj, G. Marban and A. B. Fuertes, *Nanotechnology*, **2007**, *18***,** 145603-145609.
11. Z. Gao, F. Cui, S. Zeng, L. Guo and J. Shi, *Micropor. Mesopor. Mater.*, **2010**, *132*, 188-195.
12. C. Cocozza, V. D'Orazio, T. M. Miano and W. Shotyk, *Org. Geochem.*, **2003**, *34*, 49-60.
13. L. P. C. Romao, J. R. Lead, J. C. Rocha, L. C. de Oliveira, A. H. Rosa, A. G. R. Mendonca and A. de Souza Ribeiro, *J. Braz. Chem. Soc.*, **2007**, *18(4)*, 714-720.
14. L. Rusu, M. Harja, A. I. Simion, D. Suteu, G. Ciobanu and L. Favier, *Korean J. Chem. Eng.*, **2014**, *31(6)*, 1008-1015.
15. 89-4927 ICDD, 2002 JCPDS.
16. H. P. Klug and L. E. Alexander, "X–ray diffraction procedures for polycrystalline and amorphous materials", 2nd ed. John Wiley, New York, 1974.
17. B. D. Cullity and S. R. Stock, "Elements of X-ray diffraction", Prentice Hall, NJ, 2001.
18. A. M. Dumitrescu, A. I. Borhan, A. R. Iordan, I. Dumitru and M. N. Palamaru, *Powder Technol.*, **2014**, *268*, 95-101.
19. K.S. Muthu and N. Lakshminarasimhan, *Ceram. Int.*, **2013**, *39*, 2309-2315.